Available online at www.sciencedirect.com
SCIENCE DIRECT®
Physics Letters A 326 (2004) 273–280
PHYSICS LETTERS A
www.elsevier.com/locate/pla

Optical properties of a dielectric–metallic superlattice: the complex photonic bands

D. Soto-Puebla [a,b,*], M. Xiao [c], F. Ramos-Mendieta [b]

[a] *Programa de Posgrado del Centro de Investigación Científica y de Educación Superior de Ensenada, Apartado Postal 2732, Ensenada, Baja California CP 22860, Mexico*
[b] *Centro de Investigación en Física de la Universidad de Sonora, Apartado Postal 5-088, Hermosillo, Sonora CP 83190, Mexico*
[c] *Centro de Ciencias de la Materia Condensada de la Universidad Nacional Autónoma de México, Apartado Postal 2681, Ensenada, Baja California CP 22860, Mexico*

Received 14 January 2004; received in revised form 13 March 2004; accepted 14 March 2004

Available online 20 April 2004

Communicated by V.M. Agranovich

Abstract

We have studied theoretically the photonic bands in a periodic dielectric–metallic superlattice. In the calculations the absorption in the metallic layers was taken into account using the well-known Drude model for the dielectric function, $\varepsilon(\omega) = 1 - \omega_p^2/\omega(\omega + i\gamma)$. Due to the absorption in the metallic films, the Bloch vector becomes complex for all frequencies, and the waves are evanescent. The photonic band structure is strongly modified as compared to the band structure of the nonabsorbent superlattice, mainly in the region of low frequencies $\omega < \omega_p$ where bands of odd behavior appear. We also have studied the absorption, reflection and transmission spectra of light incident on a finite superlattice. The spectra show that the complex bands, with complex wave vector and real frequency, are an appropriate resource to describe the optical properties of periodic absorbent structures.

During the last decade we have witnessed the development of new physical theories and numerical methods to describe the propagation of electromagnetic waves in periodic nonabsorbent composites [1–3]. In these *photonic crystals*, the waves undergo Bragg diffraction due to the periodicity of the index of refraction, and the solutions of the wave equation that satisfy the fundamental Bloch condition determines the eigenstates or the band structure of the systems. A band structure shows how the electromagnetic waves are transmitted as a function of frequency. A band structure of a photonic system often contains various so-called band gaps where the electromagnetic propagation is forbidden. In between the band gaps there are transmission bands where electromagnetic transmission is allowed.

In the case where all the components in the system are of nonabsorbent dielectric materials the Bloch vector is a pure real number in the frequency range of the transmission bands within the respective Brillouin

* Corresponding author.
E-mail address: dsoto@cajeme.cifus.uson.mx (D. Soto-Puebla).

0375-9601/$ – see front matter
doi:10.1016/j.physleta.2004.03.070

zone, while in the band gaps the Bloch vector becomes a complex number with its real part remaining in the limit of the Brillouin zone and imaginary part varying as a function of the frequency.

However, if one of the components in the photonic system is metallic the strong absorption in this material modifies the solutions of the wave equation. For us it is not clear if the term *band structure* preserves because the absorption breaks the concept of normal mode. There exist, however, reports that suggest the way to proceed with this type of systems. On the one hand, one can find solutions that extend infinitely in space with amplitude decaying in time (real Bloch vector K and complex frequency $\omega = \omega_{\mathrm{R}} + i\omega_{\mathrm{I}}$). On the other hand, the solutions can represent evanescent waves that decay as they penetrate into the system (complex wave vector $K = K_{\mathrm{R}} + iK_{\mathrm{I}}$ and real frequency ω). For the first case, calculations with complex frequency have shown an important role of the absorption in superlattices. Apparently it produces considerable enlarge of the band gaps [4]. With complex wave vector, the second case, the attenuation of the modes has been discussed by several authors [5–7]. Particularly in Ref. [5] different methods were used to obtain the absorption coefficient and the lifetime of the modes of propagation. The studies have been extended to systems of two- and three-dimensional periodicity (2D and 3D photonic crystals). It has been shown that small metallic inclusions in diamond and zinc-blende structures affect dramatically the photonic bands [8]. Also, new photonic states were reported under the presence of weak dissipation in systems of 2D periodicity [9].

In this Letter we present an alternative study of the complex band structure of a dielectric–metallic superlattice within the scheme of complex Bloch wave vector and real frequency. We shall establish that such a band structure describes properly the propagation and attenuation of the electromagnetic waves in finite absorbing systems. With this purpose we present the correspondence between the frequency bands and the reflection and transmission spectra for thick enough samples. In describing our solutions we shall make particular emphasis in the region of frequencies below the plasma frequency ω_{p} of the constitutive metal. We have found bands of odd behavior, to our knowledge, not previously reported. Calculation of complex bands in absorbing systems is not very popular due to the numerical complications introduced by the complex refraction index. However, the role of the absorption in transmission spectra has been discussed by several authors [10–12].

Let us begin presenting the basic formulas used for the numerical study. For structures of 1D periodicity the well-known basic equation that describes the electromagnetic modes along the lattice axis is

$$\cos(Kd) = \cos\left(n_1\frac{\omega}{c}a\right)\cos\left(n_2\frac{\omega}{c}b\right) - \frac{1}{2}\left[\frac{n_2}{n_1}+\frac{n_1}{n_2}\right] \times \sin\left(n_1\frac{\omega}{c}a\right)\sin\left(n_2\frac{\omega}{c}b\right), \tag{1}$$

where K is the Bloch vector, $d = a + b$ is the period and n_1 and n_2 are the indices of refraction of the layers of thickness a and b, respectively. Eq. (1) can be obtained via the transfer-matrix method [13,14] and is equivalent to the well established Kronig–Penney relation in the electronic problem. We assume that index n_1 is a complex function $n_1 = n_{\mathrm{R}}(\omega) + in_{\mathrm{I}}(\omega)$ which represents a metal, and the index n_2 a real number. Inputting n_1 and n_2 into Eq. (1), it takes the form

$$\cos(Kd) = f_1 + if_2, \tag{2}$$

with f_1 and f_2 real functions. Thus, solutions with complex K can be numerically obtained.

The absorption in the metallic layers is taken into account employing the Drude model for the dielectric constant

$$\varepsilon(\omega) = 1 - \frac{\omega_{\mathrm{p}}^2}{\omega(\omega + i\gamma)}, \tag{3}$$

where ω_{p} is the plasma frequency of the conduction electrons and γ the frequency of the electronic collisions. The corresponding index of refraction $n_1 = \sqrt{\varepsilon}$ has real and imaginary components. For comparison we plot in Fig. 1 the index with and without absorption for a metallic material of plasma frequency $\omega_{\mathrm{p}} = 10$ eV. In the case of absorption, for which we have chosen $\gamma = 0.1\omega_{\mathrm{p}}$, one can see from Fig. 1 that the real part is strongly distorted in the regime of low frequencies.

It is constructive to analyze the behavior of the functions f_1 and f_2 involved in Eq. (2) (we are not

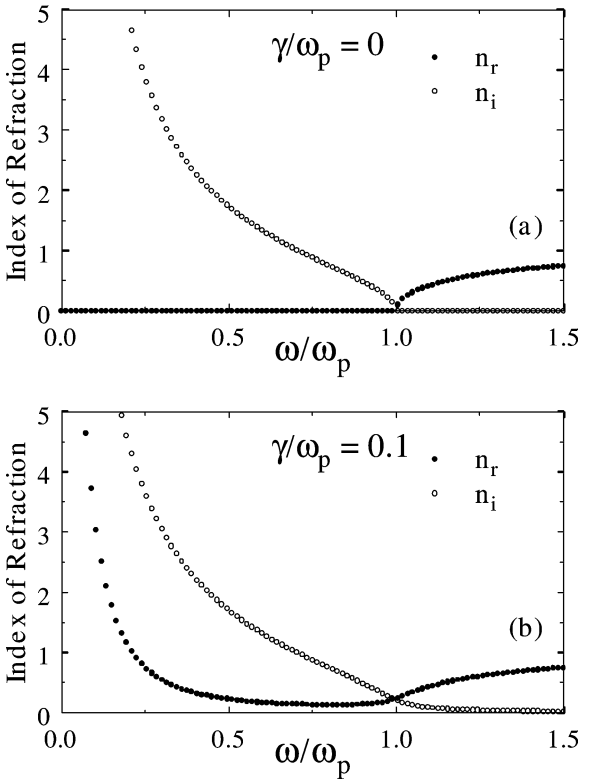

Fig. 1. Dependence of the index of refraction n on the absorption coefficient γ. Through all of this Letter the plasma frequency has the value $\omega_p = 10$ eV ($\sim 15 \times 10^{15}$ s^{-1}).

showing the form of these functions because of the simplicity of the algebra involved to obtain them). We have chosen for the superlattice the relation $a/b = 0.1$, with $d = 100$ nm. The metal is the same of Fig. 1; the dielectric layer is air, $n_2 = 1$. Fig. 2 shows the functions for the particular case $\gamma = 0$. As is expected $f_2 = 0$ $\forall\omega$ and f_1 oscillates defining the frequency regions in which the argument Kd takes real values (the regions where $|f_1| \leqslant 1$). It can be seen that the first and second allowed bands are defined by the intervals $0.29 \leqslant \omega/\omega_p \leqslant 0.62$ and $0.75 \leqslant \omega/\omega_p \leqslant 1.24$, respectively.

When absorption is included the functions f_1 and f_2 are strongly modified, particularly in the region of low frequencies $\omega \ll \omega_p$, as is shown in Fig. 3. In this region, determined by the damping constant γ, the filling fraction and the period length, the functions f_1 and f_2 change from oscillatory and tend to the limit values one and zero, respectively. (The values of this

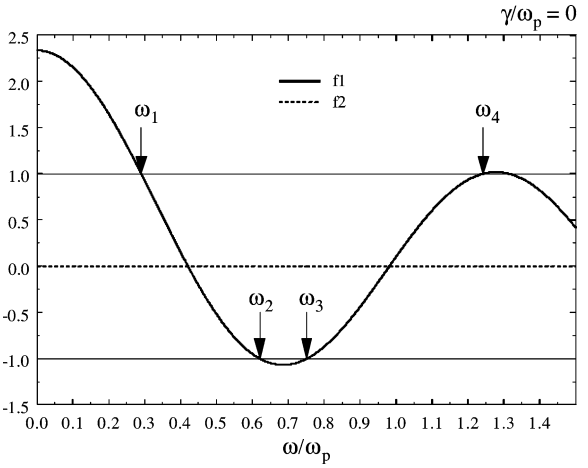

Fig. 2. The functions f_1 and f_2 associated to a nonabsorbent superlattice.

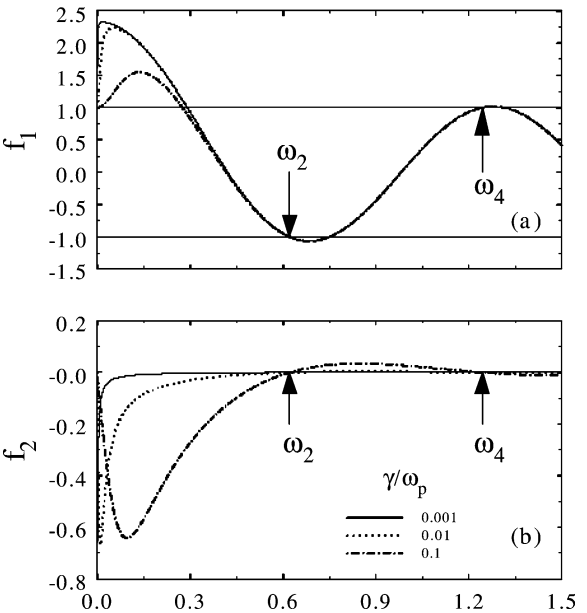

Fig. 3. The functions f_1 and f_2 associated to an absorbent superlattice. We plot the curves for four values of the absorption parameter γ.

limits differ from those presented in Ref. [5] where the real part satisfies $f_1(\omega \to 0) < 1$. Consequently our solutions do not coincide with the results shown in such article. As we shall see, a careful analytical and numerical treatment of Eq. (1) leads to complex solutions whose frequency structure *does not present* band gaps, as was reported in Ref. [5].) Another

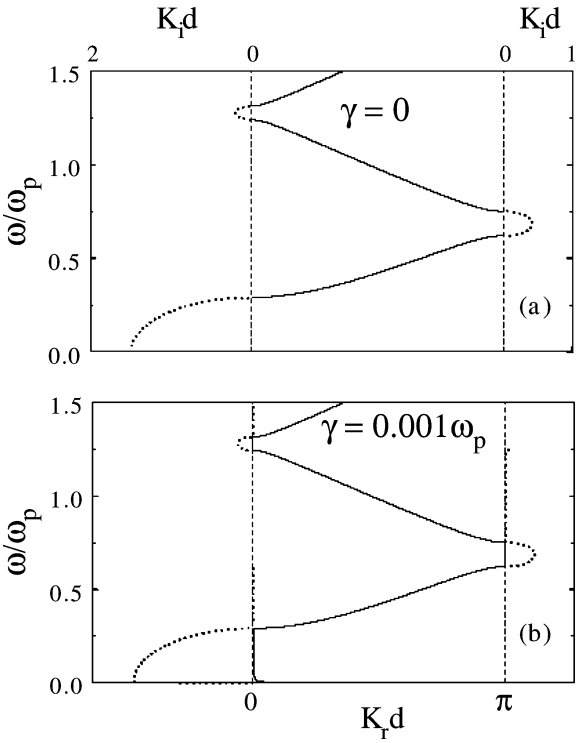

Fig. 4. The photonic band structure. (a) The system is constituted by alternated air and dispersive nonabsorbent layers, the latter of dielectric function $\varepsilon(\omega) = 1 - \omega_p^2/\omega^2$. (b) The same as (a) but now the dispersive layers include small absorption effects. The metallic filling fraction is $f = 0.1$ and the cell size is $d = 100$ nm.

particularity is that the curves of f_1 for different values of γ cross just at the frequencies ω_2 and ω_4, the upper edges of the first and second bands. In the crosses $f_1 = \pm 1$. A similar behavior occurs to the curves of f_2, but at the cross points $f_2 = 0$. It means that at these particular frequencies, ω_2 and ω_4, the dispersion relations $\omega(K)$ of the waves in the superlattice, either with or without absorption, coincide.

Now we present the numerical solutions of Eq. (2). Fig. 4 shows the effect of dissipation on the band structure. With $\gamma = 0$ (see Fig. 4a) the curves have the expected form. As the frequency increases the Bloch vector that defines the modes changes from complex to real and from real to complex, and so on. The highest imaginary vector in each gap coincides with the corresponding mid-frequency gap except in the lowest gap. Fig. 4b shows that the small perturbation $\gamma = 0.001\omega_p$ already produces a noticeable modification of the structure at low frequencies. In the first gap a small real wave vector arises with an odd behavior in the region of low frequencies and the imaginary component deforms penetrating with finite amplitude into the region of the first allowed band. Thus, the first allowed band no longer represents pure modes of propagation at least at the lower edge where the modes are now attenuated. In the second and third gaps only a tiny real wave vector appears while the imaginary component remains practically unchanged.

With higher γ the band structure undergoes a strong deformation as is shown in Fig. 5 where we present the bands for $\gamma = \{0.01, 0.1\}\omega_p$. With $\gamma = 0.1\omega_p$, the curve of real vectors backbends. This type of effect is well known in physics of surface plasmons [15]. Of course that the bands of Fig. 3 do not stem from the coupling of surface plasmons (we are considering propagation only on the direction of periodicity). However, the modes at frequencies below the plasma frequency have fields that decay exponentially inside each metallic layer, the similar requirement for the occurrence of surface plasmons. The backbending effect, that appears already for $\gamma = 0.001\omega_p$, results from the boundary conditions that the fields satisfy at each interface dielectric–metal at frequencies below ω_p. Some time ago several authors have discussed the involved physics for single interfaces [16]. However, additional study is now required in order to determine the role played by the periodicity.

Fig. 5 shows that as γ is increased the backbending tends to disappear. Note the reader that the frequencies of the upper band edges for $\gamma = 0$ (see Fig. 4) remain as the reflection points of the dispersion curves at the limit of the Brillouin zone when $\gamma \neq 0$. The existence of these fixed points was already predicted from the analysis of the functions f_1 and f_2 above.

Figs. 4 and 5 show that absorption breaks the concept of band structure (as a series of allowed and forbidden frequency regions). However, some properties of the electromagnetic waves in a semiinfinite superlattice can be established from the complex solutions. In the region of the original ($\gamma = 0$) lowest gap, $0 \leqslant \omega/\omega_p \leqslant 0.29$, we found that the Bloch vector develops a real component K_R. We also see that as higher γ lower the imaginary component K_I (see K_I at the mid frequency of the gap). Thus, in a semiinfinite sample the waves penetrate more (beyond they penetrate in absence of losses) presenting an additional oscillatory behavior introduced by K_R that tends to break

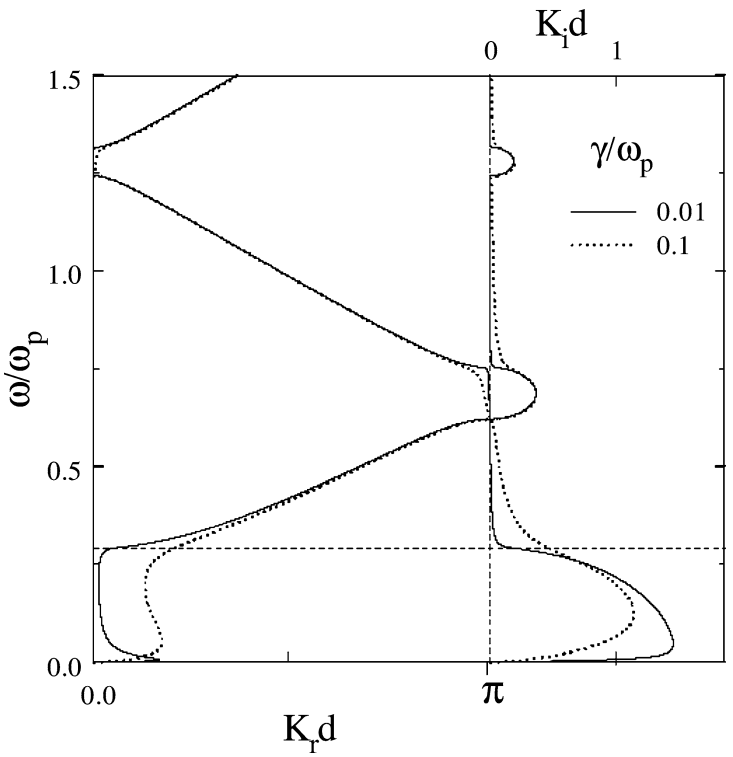

Fig. 5. The complex bands as function of γ. Strong deformation of the curves is observed mainly in the regime of lower frequencies.

the standing wave conditions of the original gap. Low metallic absorption only perturbs the standing waves; a perturbed gap remains—no oscillatory waves are expected to traverse thick enough finite samples.

Contrarily, in the region of the first original allowed band $0.29 \leqslant \omega/\omega_{\mathrm{p}} \leqslant 0.62$, the conditions for complete propagation in absence of losses is now perturbed. In a semiinfinite sample the oscillatory waves penetrate but now due to the presence of absorption they acquire an exponential envelop that decays into the sample. The shorter penetration distance δ (distance at which an incident wave decay to $1/e$ of its value at a surface), the higher imaginary K_{I}. Fig. 5 shows that the upper band edge is less sensitive to the metallic losses. In fact the original upper band edge (with $\gamma = 0$) at the zone border preserves. Similar effect has been also reported for 2D systems and have to do with the behavior of the standing waves near the gap borders. From the band structure we conclude that in the upper edge of the first band the fields are mostly localized at the dielectric region (the effect of the absorption is almost negligible). At the lower band edge, however, the fields are localized at the metallic films giving rise to considerable absorption.

We may give similar description of the complex bands in regions corresponding to upper forbidden and allowed original bands. Our conclusions are, on the one hand, the metallic absorption affects the standing wave conditions in the band gaps increasing the wave penetration of an incident wave (the bands develop a real vector component). For a semiinfinite superlattice (or a thick enough superlattice slab) this additional penetration produces field evanescence due to the metallic losses (as higher the penetration, higher the probability of absorption of the incident wave). On the other hand, as is expected, the metallic absorption adds a decaying behavior to the original oscillatory solutions. In this case the interesting point is the asymmetry of the penetration distance δ; short at low frequencies, long at high frequencies, in the same allowed band.

Next we present the optical response of a finite multilayer. The sample, of material parameters the same of the superlattice treated above, is constituted

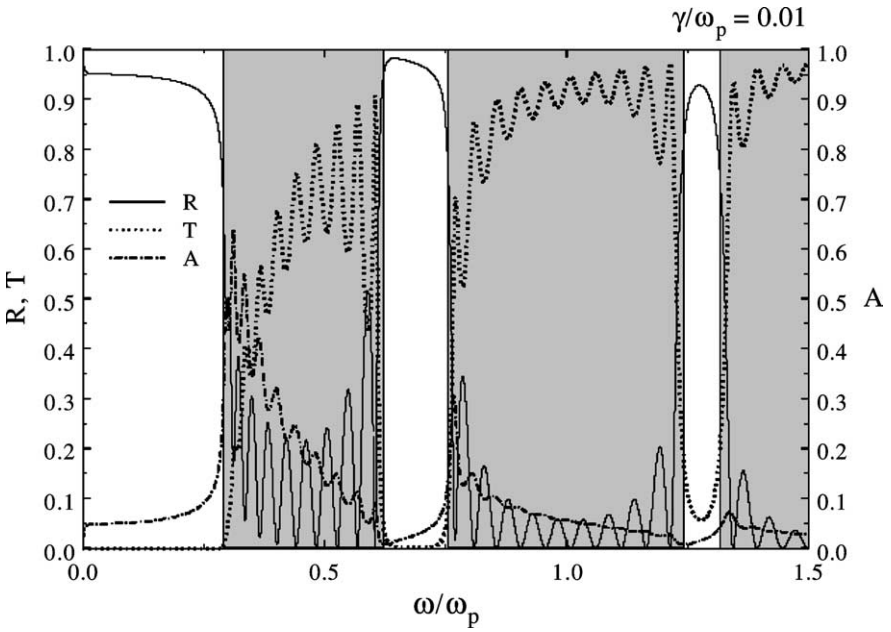

Fig. 6. R, T and A spectra corresponding to a finite multilayer of 11 cells. These functions satisfy $R + T + A = 1$. The shaded regions represent allowed bands of the nonabsorbent system. Absorption is higher at the lower band edges.

by 11 cells (22 layers) and the incident and the transmitted media are air. This is a thick enough sample for which the reflection (R), transmission (T) and the multilayer absorption (A) of the normally incident wave are expected to be in agreement with the complex photonic bands. The ordinary transfer matrix methods were employed in these calculations.

Small loss in the metallic layers distorts the well-known R, T and A spectra of a nonabsorbent multilayer (not shown here). With $\gamma = 0.01\omega_p$ Fig. 6 shows that the first gap remains for T even when $R < 1$. Finite absorption appears increasing as the frequency approaches to the first band. Note that the three functions R, T and A do not oscillate in this region. The waves are stationary with some degree of perturbation that causes wave absorption. The high absorption at the gap edge is in agreement with the large imaginary vector component observed in the band structure.

Then, inside the first allowed band we observe ordinary Fabry–Perot oscillations (the main characteristic of oscillatory modes in finite systems). The reflectivity appears symmetric with respect to the band edges but, contrarily, the transmittance is low at the lower band edge and high at the higher band edge. The profiles of R and T indicate that T is more sensitive to the superlattice absorption, which is higher at the lower band edge (see Fig. 6). Note that peaks of A coincide with the peaks of T.

On the other hand, the second gap seems almost the same of the nonabsorbent case, only with an small increasing absorption. In the third gap R and T show already the effects of finite structure with an additional small absorption. Fig. 6 also shows that the superlattice absorption is strongly reduced in the second and third allowed bands.

The results presented in Fig. 6 are in complete correspondence with the complex bands of Fig. 4b. A small real wave vector component in the gaps perturbs the standing wave conditions giving rise to finite absorption; then, a small imaginary wave vector component in the allowed bands means the waves decay by absorption. It is very important to remark that the spectra shown in Fig. 6 represent a small modification of the spectra corresponding to the nonabsorbent structure. For the wave transmittance the band gaps are essentially unaltered.

Now we refer to Fig. 7. As can be seen with $\gamma = 0.1\omega_p$ the R, T and A spectra are strongly perturbed, particularly in the region $\omega < \omega_p$. The

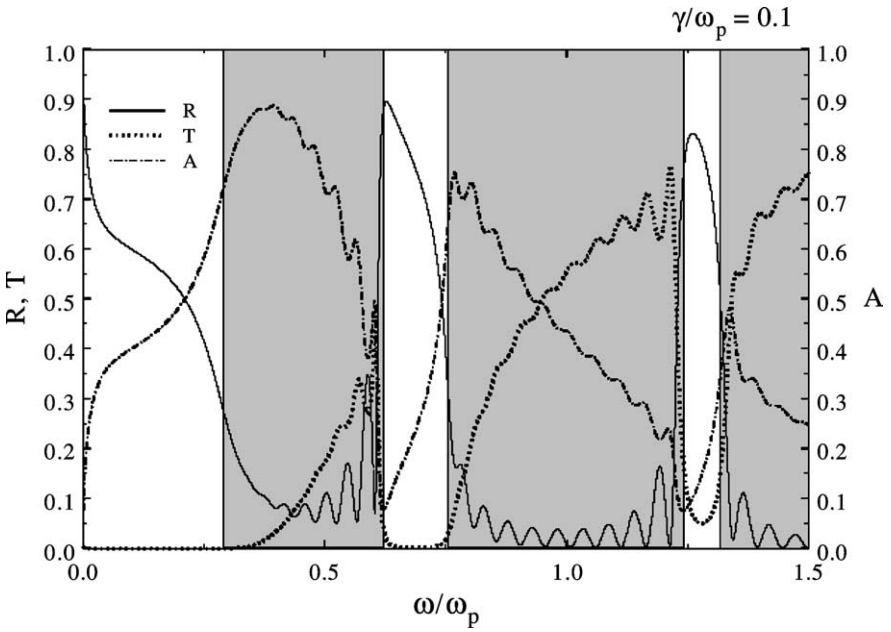

Fig. 7. The same as Fig. 6 but realistic the metallic absorption. The slope variation of A in the first gap reflects the backbending structure of the bands. Fabry–Perot oscillations (transmission) begin at a frequency inside the first gap. The first transmission gap is enlarged.

backbending effect of the bands gives to R and A variable slope inside the first gap. We also observe an enlarge of the lowest transmission gap. Note that transmission begins at a frequency inside the original allowed band almost coinciding with the absorption maximum. At such a frequency A (R) modifies its behavior from monotonically increasing (decreasing) to an oscillatory one—the Fabry–Perot oscillations. As higher the metallic absorption we found that transmission begins at higher frequencies.

In spite of the T asymmetry in the allowed bands, Fig. 7 shows that realistic metallic absorption leaves the structures of R and T with some remnant of the original (without absorption) band structure. The frequencies at which the second and third gaps begin are practically unaltered.

We know that R, T and A depend on the thickness D of the superlattice slab. With help of the complex bands one may estimate D in order to obtain a desirable transmission. For example, at the center of the first band ($\omega/\omega_p = 0.45$) with $\gamma = 0.1\omega_p$ we found from Fig. 5 that $K_I = 9.7 \times 10^{-4}$ nm^{-1}. Thus, for our sample of eleven cells at such frequency we have $\exp(-K_I D) \sim \exp(-1)$. It means that $D \sim \delta$ and transmittance is expected (as effectively it occurs. See Fig. 7). However at the lower edge ($\omega/\omega_p = 0.29$), $K_I = 4.7 \times 10^{-3}$ nm^{-1} and $\exp(-K_I D) \sim \exp(-5)$. It corresponds to a very low transmission not appreciable in the scale of Fig. 7.

Now we make some final remarks. In treating the problem of absorption in 2D and 3D photonic crystals with metallic components previous reports have speculated about new states inside the band gaps [9]. From our calculations we concluded that no similar states appear in 1D systems. We have found that inside the gaps the waves may penetrate more in presence of absorption but not as an eigenstate of propagation (there exists an imaginary Bloch vector component that makes the wave evanescent). On the other hand, the complex band structure here reported leaves diffuse the lower edge of the frequency regions of mainly oscillatory solutions. However, the upper edge, the point of maximum oscillation, is clearly established at the border of the Brillouin zone. At such points, the imaginary component of the wave vector is minimum; the waves propagate almost without damping. Thus, the complex bands allows one to know the frequency regions at which the higher transmission is expected through finite samples.

It is important to say that previous reports of calculations in the scheme of complex frequency and real wave vector have found considerable enlarge of some photonic gaps due to the presence of absorption [4]. Now, within the scheme of complex wave vector and real frequency, we cannot speak of an absolute enlarge of the band gaps. As Fig. 7 shows, apparently the first band gap for T enlarges and the gap edge penetrates into the region of the first allowed band. However, this is a relative result because the frequency at which appreciable transmission begins depends on the number of cells in the sample. As thicker the sample, higher the frequency of threshold for transmittance. For example, with a multilayer of eleven cells finite transmission exist only at frequencies higher than $\omega \sim 0.40\omega_p$; with twenty cells this frequency moves to $\omega \sim 0.50\omega_p$ and, for forty cells transmission begins at $\omega \sim 0.59\omega_p$. It means that for the sample of forty cells the lowest gap is defined by $0 < \omega/\omega_p < 0.59$ while for the sample of eleven cells it has the frequencies $0 < \omega/\omega_p < 0.40$. Thus, with respect to a nonabsorbent multilayer, the lowest gap for T is enlarged by the absorption in finite systems. All of this behavior can be inferred from the complex band structure.

We want to remark that the metallic losses make complex the Bloch wave vector. It means that the correct description of the wave propagation is given by the two wave vector components, real and imaginary. One cannot speak of a *real* band structure $\omega = \omega(K_R)$. For this reason we believe that the band structure reported by other authors, particularly in Ref. [5], need be reconsidered.

In conclusion, we have presented the complex bands that describe the electromagnetic wave propagation in dielectric–metallic superlattices. The loss mechanisms in the metallic layers modify the well-known structure of allowed and forbidden frequency ranges of the corresponding nonabsorbent multilayer. Due to the presence of a finite imaginary Bloch vector component our solutions have physical sense only for finite systems. We found that the metallic absorption perturbs the conditions for stationary waves allowing higher penetration (shorter imaginary K_I) of the waves at frequencies of the nonabsorbent multilayer gaps. The higher penetration is accompanied of higher absorption. The complex bands define clearly the frequency regions where highest transmission through a finite sample is expected.

Acknowledgements

This work was supported by Consejo Nacional de Ciencia y Tecnología, CONACyT México, Grant No. 489100-5-3554-E. D.S.P. is grateful to CONACyT and PROMEP (Programa de Mejoramiento del Profesorado de la Secretaría de Educación Pública, México) for support.

References

[1] J.D. Joannopoulos, R.D. Meade, J.N. Winn, Photonic Crystals: Molding the Flow of Light, Princeton Univ. Press, Princeton, 1995.
[2] K. Sakoda, Optical Properties of Photonic Crystals, in: Springer Series in Optical Sciences, Springer, 2001.
[3] S.G. Johnson, J.D. Joannopoulos, Photonic Crystals (The Road from Theory to Practice), Kluwer Academic Publishers, Boston, 2002.
[4] A. Moroz, A. Tip, J.M. Combes, Synth. Met. 116 (2001) 481.
[5] V. Kuzmiak, A.A. Maradudin, Phys. Rev. B 55 (1996) 7427.
[6] M.M. Sigalas, C.M. Soukoulis, C.T. Chan, K.M. Ho, Phys. Rev. B 49 (1994) 11080.
[7] M. Xiao, Mater. Lett. 56 (2002) 945.
[8] A. Moroz, Phys. Rev. B 66 (2002) 115109.
[9] A.A. Krokhin, P. Halevi, Phys. Rev. B 53 (1995) 1205.
[10] N. Stefanou, V. Karathanos, A. Modinos, J. Phys.: Condens. Matter 4 (1992) 7389.
[11] V. Yannopapas, A. Modinos, N. Stefanou, Phys. Rev. B 60 (1999) 5359.
[12] R.C. McPhedran, N.A. Nicorovici, L.C. Botten, C. Martijn de Stertke, P.A. Robinson, A.A. Asatryan, Opt. Commun. 168 (1999) 47.
[13] F. Abelés, Ann. Physique 5 (1950) 596.
[14] P. Yeh, Optical Waves in Layered Media, Wiley, New York, 1988.
[15] J.B. Pendry, J. Mod. Opt. 41 (1994) 209.
[16] A.D. Boardman (Ed.), Electromagnetic Surface Modes, John Wiley and Sons, New York, 1982.